Causal Set Theory

A Statistical Perspective

Nikshay Chugh[1] under supervision of Deepak Dhar[2]

[1]Indian Institute of Science

[2]International Centre for Theoretical Sciences

PSI Start, June 2025

Outline

(1+1)D Minkowski Spacetime Setup

- Consider flat $(1+1)$D spacetime with coordinates (t, x)
- Diamond-shaped region with vertices:
  - $(0,0)$, $(T/2, T/2)$, $(-T/2, T/2)$, $(0, T)$
- Sample N events uniformly at random
- Construct causal set [1, 2, 3] $\mathcal{C} = \{\text{events in diamond}\}$

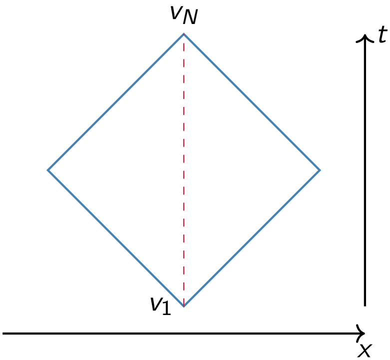

Figure: A causal diamond with minimal and maximal element

Partial Order Relations

A causal set $(\mathcal{C}, \prec)$ requires a partial order relation $\prec$ that is:

1. **Reflexive**: $v_x \prec v_x$ for all $v_x \in \mathcal{C}$
2. **Antisymmetric**: If $v_x \prec v_y$ and $v_y \prec v_x$, then $v_x = v_y$
3. **Transitive**: If $v_x \prec v_y$ and $v_y \prec v_z$, then $v_x \prec v_z$
4. **Locally finite**: Finite number of events between any two causally related events

The relation $\prec$ encodes the **causal structure** of spacetime events.

We do not need **local finiteness** to construct a poset, but since we need a discrete poset we apply such a restriction.

The Coordinate Assignment Problem [4, 5]

Initial Question

Given causal set $(\mathcal{C}, \prec)$, can we assign unique coordinates to events in flat $\mathbb{M}^2$ Minkowski spacetime?

The Coordinate Assignment Problem [4, 5]

Initial Question

Given causal set $(\mathcal{C}, \prec)$, can we assign unique coordinates to events in flat $\mathbb{M}^2$ Minkowski spacetime?

Answer: No - infinitesimal coordinate changes preserve causal structure

The Coordinate Assignment Problem [4, 5]

Initial Question

Given causal set $(\mathcal{C}, \prec)$, can we assign unique coordinates to events in flat $\mathbb{M}^2$ Minkowski spacetime?

Answer: No - infinitesimal coordinate changes preserve causal structure

Refined Question

Can we assign coordinates up to finite precision?

The Coordinate Assignment Problem [4, 5]

Initial Question

Given causal set $(\mathcal{C}, \prec)$, can we assign unique coordinates to events in flat $\mathbb{M}^2$ Minkowski spacetime?

Answer: No - infinitesimal coordinate changes preserve causal structure

Refined Question

Can we assign coordinates up to finite precision?

Still problematic - Lorentz transformations and coordinate shifts preserve causal structure

The Coordinate Assignment Problem [4, 5]

Initial Question

Given causal set $(\mathcal{C}, \prec)$, can we assign unique coordinates to events in flat $\mathbb{M}^2$ Minkowski spacetime?

Answer: No - infinitesimal coordinate changes preserve causal structure

Refined Question

Can we assign coordinates up to finite precision?

Still problematic - Lorentz transformations and coordinate shifts preserve causal structure

Well-Defined Question

Given causal set $(\mathcal{C}, \prec)$ with fixed minimal/maximal elements $v_{\min}, v_{\max}$ in flat $\mathbb{M}^2$, can we assign coordinates up to finite precision?

Answer: Yes!

Causal Set Structures

Define important causal structures for event v_x:

$$J^+(v_x) = \{v_y \in \mathcal{C} \mid v_x \prec v_y\} \quad \text{(future light cone)} \tag{1}$$
$$J^-(v_x) = \{v_y \in \mathcal{C} \mid v_y \prec v_x\} \quad \text{(past light cone)} \tag{2}$$
$$L_c(v_x) = J^+(v_x) \cup J^-(v_x) \quad \text{(light cone)} \tag{3}$$
$$[v_x, v_y] = J^+(v_x) \cap J^-(v_y) \quad \text{(Alexandrov interval)} \tag{4}$$

The **Alexandrov interval** $[v_x, v_y]$ contains all events causally between v_x and v_y.

Lorentz Invariance

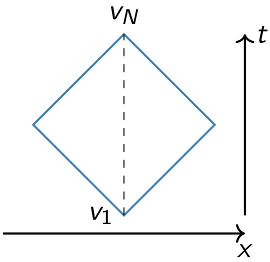

Figure: Original Frame

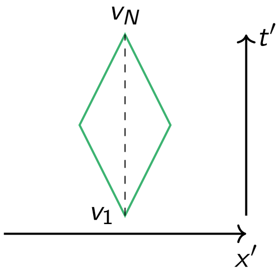

Figure: Boosted Frame

- Proper volume of diamond region is Lorentz invariant
- Uniform (Poisson) sampling maintains Lorentz invariance
- Causal structure preserved under boosts

Accessible Events and Proper Time

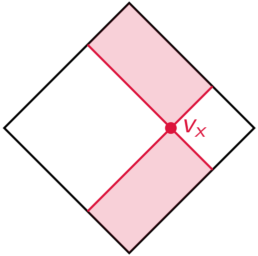

Key Insight:

- Fewer events accessible to v_x than to minimal element v_1
- Number of accessible events $\propto$ proper time measure
- Each **step** to nearest future event $\sim$ unit proper time

Hasse Diagrams

Minimal graphical representation of partial order

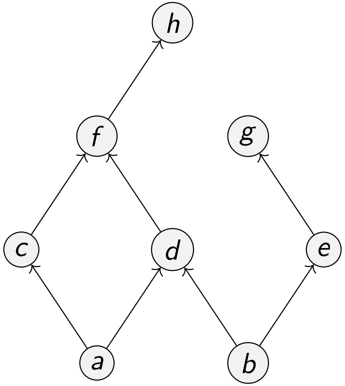

Figure: Hasse diagram of 8 elements

Properties:

- Directed Acyclic Graph (DAG)
- Only direct connections shown
- Transitivity implied
- Non-comparable pairs: (a, b), (c, d), (d, e), etc.

Proper Time:

- $t_{\text{link}} = 1$
- Natural discretization

Breaking Symmetries

Problem: Causal structure alone is insufficient - need to fix symmetries

1. **Translation invariance**: Fix $v_1 \mapsto (0,0)$ (anchor point)
2. **Parity invariance**: Choose light propagation direction
3. **Lorentz invariance**: Fix $v_N \mapsto (0,T)$ (time coordinate)

Embedding map: $p : \mathcal{C} \to \mathbb{M}^2$ with $p(v_1) = (0,0)$ and $p(v_N) = (0,T)$

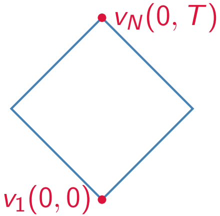

Figure: Skeleton of the embedding

Causal Relations and Proper Time

Causal condition: For $v_x \prec v_y$ in $\mathbb{M}^2$: $x^0 \leq y^0 \quad \text{and} \quad (y^0 - x^0)^2 - (y^1 - x^1)^2 \geq 0$

Proper time for timelike separation: $\tau(y^\mu, x^\mu) = \sqrt{(y^\mu - x^\mu)(y_\mu - x_\mu)}$

Event density: For diamond volume $T^2/2$ with N events: $\rho = \frac{2N}{T^2}$

General dimension: $c_d \cdot T^d \cdot \rho = N$ where $c_2 = 1/2$

Two Definitions of Proper Time

For causally related events $v_x \prec v_y$:

1. **Geodesic-inspired** (τ_G):

$$C(v_x, v_y) = \{\text{chains between } v_x \text{ and } v_y\} \tag{5}$$

$$\tau_G(v_x, v_y) = \max_{\zeta \in C(v_x, v_y)} |\zeta| \tag{6}$$

   Length of maximal chain (longest causal path)

2. **Alexandrov interval-inspired** (τ_A):

$$\tau_A(v_x, v_y) = \left(\frac{|[v_x, v_y]|}{c_d \cdot \rho} \right)^{1/d} \tag{7}$$

   Based on volume of Alexandrov interval

Boundary condition: $\tau_G(v_1, v_N) = \tau_A(v_1, v_N) = T$

Causal Set Geometry

Triangle relations: For $v_x \prec v_y \prec v_z$

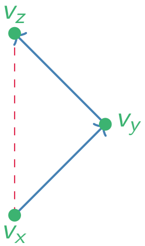

Figure: Three elements of the causet

Causal contraction:

$$\langle v_z - v_x | v_z - v_x \rangle_{\mathcal{C}} := \frac{1}{2}[\tau(v_x, v_z)^2 - \tau(v_x, v_y)^2 - \tau(v_y, v_z)^2] \tag{8}$$

Time coordinate: $t(v_x) = \frac{T}{2} + \frac{\tau(v_1, v_x)^2 - \tau(v_x, v_N)^2}{2T}$

Spatial Coordinate Reconstruction

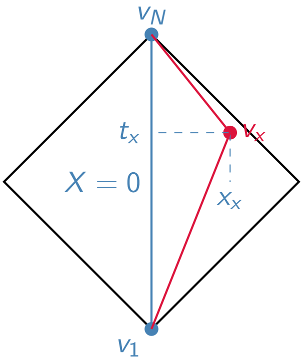

Figure: Pythogorean construction

Spatial coordinates from:

$$\left(\frac{T}{2} - t(v_x)\right)^2 + x(v_x)^2 = -\tau(v_x, v_N)^2 \tag{9}$$

$$\left(\frac{T}{2} + t(v_x)\right)^2 + x(v_x)^2 = -\tau(v_1, v_x)^2 \tag{10}$$

Parity resolution:

- Two solutions: $\pm x(v_x)$
- Symmetric distribution about $X = 0$
- Assign based on density balance

Antichains and Spacelike Separation

Antichain: Set of mutually incomparable elements
For events v_x, v_y, define:

$$\mathfrak{p}(v_x, v_y) = \{v_z \in J^-(v_x) \cap J^+(v_y) \mid \max(t(v_z))\} \quad (11)$$
$$\mathfrak{f}(v_x, v_y) = \{v_z \in J^+(v_x) \cap J^-(v_y) \mid \min(t(v_z))\} \quad (12)$$

Spacelike separation measure: $I(v_x, v_y) := \tau(\mathfrak{p}(v_x, v_y), \mathfrak{f}(v_x, v_y))$

- Proper time when $v_x \prec v_y$
- Spacelike separation when incomparable
- Enables complete coordinate reconstruction

Maximal Chain Assignment of Coordinates

- **Goal:** Assign coordinates to causal set events using maximal chains
- **Method:** Uniformly distribute maximal chain on line from v_1 to v_N
- **Expectation:** Unique maximal chain exists (choose one if multiple)
- **Symmetry:** Event distribution symmetric about $X = 0$ line

Iterative Process

1. Assign time coordinate to maximal chain
2. Move to next pair of maximal chains
3. Continue until reaching maximally spacelike separated events

Dimensional Analysis

- In flat spacetime with d spatial dimensions: expect d next-maximal chains
- **Natural interpretation:** Number of next-maximal chains $=$ spatial dimensions
- **Key question:** Can we determine embedding dimension from causal set?

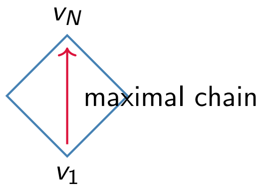

Tolerance in Chain Length

- **Problem:** Maximal chain length may not be unique
- **Solution:** Introduce tolerance ϵ for chain length deviation
- **Physical interpretation:**
  - May relate to system physics
  - In quantum systems: connection to uncertainty principle

Mathematical Formulation

Allow chains with length $L_{\max} - \epsilon \leq L \leq L_{\max}$

Path Shape Problem

- Two paths P_1, P_2 with same length but different shapes:
  - P_1: Nearly straight, small X-deviations
  - P_2: Zig-zag, large X-deviations
- **Question:** Which path to choose as maximal chain?
- Current method ignores path shape
- Overlapping points create ambiguity

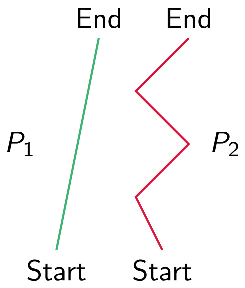

Local Substructure Challenge

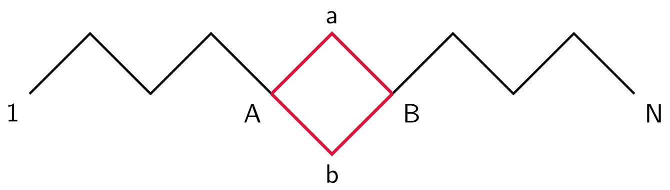

- **Problem:** Different paths lead to intermixing of events *a* and *b*
- Coordinate assignment becomes ambiguous in plaquette regions
- This feature is inherent to the theoretical framework

Expected Regions: Voronoi Tessellation

- **Question:** We want to decompose spacetime into cells such that there is exactly one point per cell. Some more constraints if needed.
- **Answer:** Use Voronoi tessellation
- Each region contains points closer to given event than any other
- Provides statistical expectation for event locations

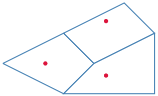

Voronoi cells

Hexagonal Structure Analysis

Using Euler's formula in 2D: $F + V - E = 2$

- Each vertex connects to 3 edges (Delaunay triangulation)
- Each edge shared by 2 vertices
- In large E limit: $E = 3F$

Result

- Average edges per Voronoi cell: 6
- **Expected shape:** Hexagonal regions in large density limit

Cell Size

- Diamond area: $T^2/2$
- Number of events: N
- Average hexagon area: $\frac{T^2}{2N}$ (determined by event density)

CausalDiamond Class Implementation

- Python implementation available on GitHub
- **CausalDiamond** class handles:
  - Point sprinkling in causal diamond
  - Causal set construction
  - Coordinate assignment using both t_G and t_A methods

Point Distribution in Causal Diamond

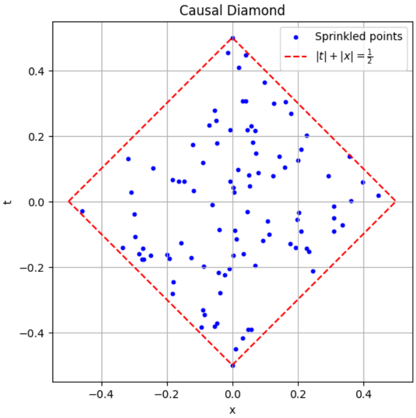

- 100 points sprinkled uniformly in causal diamond
- Forms basis for coordinate assignment comparison

Geodesic Proper Time Assignment (t_G)

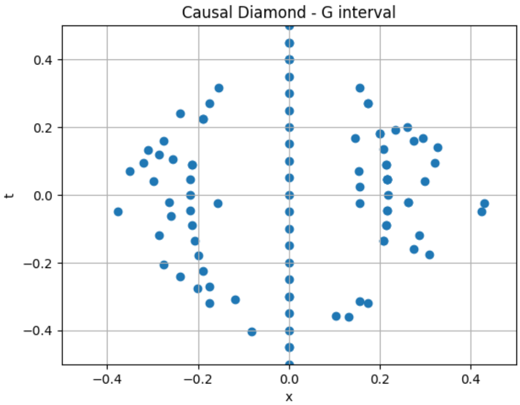

- **Key observation:** Aligns with maximal chain method
- Events equally spaced on $X = 0$ line
- Maximal chain assignment roughly unique across realizations

Alexandrov Proper Time Assignment (t_A)

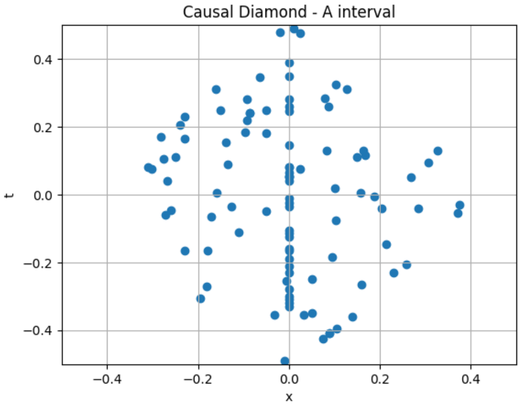

- More uniform event distribution
- Less regular spacing on $X = 0$ line
- Both methods yield maximal chain length $\sim (2N)^{1/2}$

Method Comparison

t_G **Prescription:**

- Used for dynamics/actions in CST
- Regular maximal chain structure
- Links to geometrodynamic theory
- Non-local but computationally tractable

t_A **Prescription:**

- Used for causal set geometry
- More uniform coordinate distribution
- Better geometric fidelity
- Lower variance in assignments

Unexpected Result

t_G prescription spectacularly aligns with maximal chain method

Dimension Estimators

1. **Maximal Chain Length:**
   - For d-dimensional spacetime: $L \sim (N/c_d\rho)^{1/d}$
   - c_d: dimension-dependent constant, ρ: event density
   - Approaches limit from below for large N
2. **Myrheim-Meyer Dimension [6]:**
   - Distribution of chain lengths vs. length
   - Characteristic signatures for each dimension
3. **Midpoint-Scaling Dimension [7]:**
   - Based on Alexandrov proper time between extremal elements

This can be extended to spacetimes with constant cosmological constants as well.

Distance Distribution Analysis

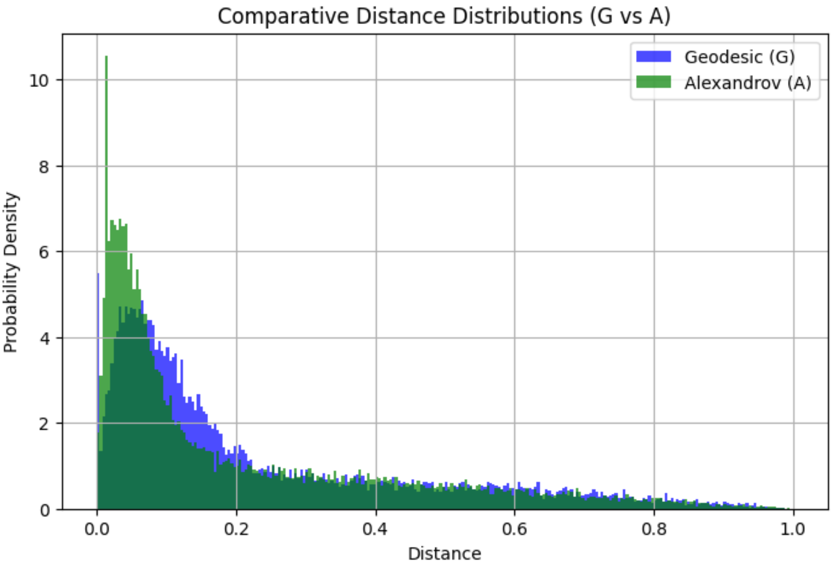

Statistical Performance Comparison

- **Distance metric:** Euclidean distance between assigned and original coordinates
- **Analysis:** Averaged over 200 realizations

Key Findings

- t_A prescription: Lower mean distance error
- t_A prescription: Lower variance in assignments
- **Conclusion:** t_A method provides better geometric fidelity

t_G Method Value

Despite lower performance, t_G remains crucial for:

- Curvature description via link counting
- Non-local action formulations for path integrals
- Sequential causal set growth modeling

Goals and Approach

- **Objective:** Compute expectation value of maximal chain length analytically
- **Method:** Hand calculation using Hasse diagrams for small N
- **Key insight:** $(2N)^{1/2}$ scaling approached strictly from below
- **Challenge:** Rapid growth in complexity for $N \geq 4$

Setup

- Causal diamond with side length $= 1$ (area $= 1$)
- Maximal chain length $=$ number of links $+ 1$
- Systematic enumeration of all possible causal sets

N=1: Trivial Case

- Single possible causal set: one event
- Maximal chain length: 1
- Probability: 1

Single event

N=2: First Non-trivial Case

Chain length 2

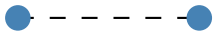

Chain length 1

- Two possible configurations
- By symmetry: equal probability $= 1/2$
- Average chain length: $\frac{2+1}{2} = 1.5$

N=2: Probabilistic Analysis

For point at (x, y) in diamond:

$$\mathbb{P}(\text{causal relation}) \tag{13}$$
$$= \int_0^1 \int_0^1 [xy + (1-x)(1-y)]\, dx\, dy \tag{14}$$
$$= 1/2 \tag{15}$$

$$\mathbb{P}(\text{no causal relation}) \tag{16}$$
$$= \int_0^1 \int_0^1 [(1-x)y + x(1-y)]\, dx\, dy \tag{17}$$
$$= 1/2 \tag{18}$$

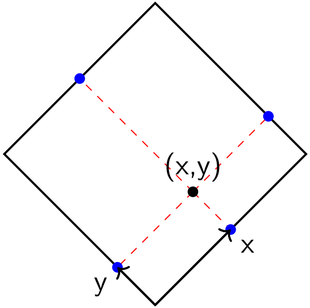

Figure: A point in the causal diamond

N=3: Growing Complexity

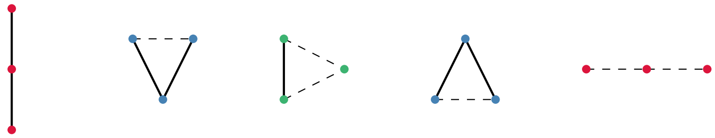

Length 3 Length 2u Length 2 Length 2d Length 1

- **Symmetries:** $\mathbb{P}(\text{length } 3) = \mathbb{P}(\text{length } 1)$
- $\mathbb{P}(\text{length } 2\text{u}) = \mathbb{P}(\text{length } 2\text{d}) = \mathbb{P}(\text{length } 2)$
- Constraint: $3\mathbb{P}(\text{length } 2) + 2\mathbb{P}(\text{length } 3) = 1$

N=3: Explicit Calculation

- Partition diamond into 9 regions for 3-point configurations
- Use integral method similar to N=2 case
- **Results:**
  - $\mathbb{P}(\text{length } 3) = 1/3$
  - $\mathbb{P}(\text{length } 2) = 1/9$
  - Average maximal chain length $= 2$

Pattern Emergence

- N=1: Average length $= 1 < \sqrt{2}$
- N=2: Average length $= 1.5 < 2$
- N=3: Average length $= 2 < \sqrt{6} \approx 2.45$
- Approaching $(2N)^{1/2}$ from below

N=4: Computational Challenge

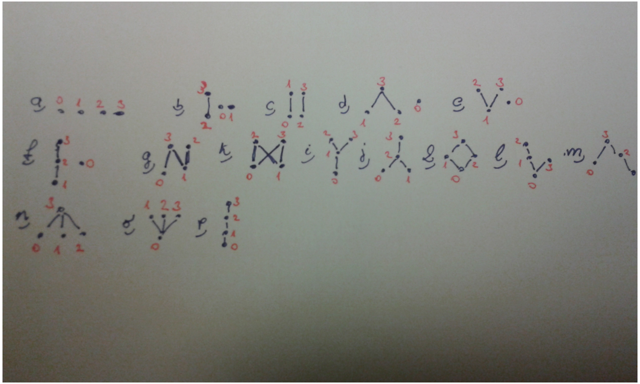

- Rapid growth in number of possible posets
- Hand calculation becomes intractable
- **Question:** How to enumerate partial orders on N-element sets?
- **Answer:** Kleitman-Rothschild approximation methods

Key Insights

- **Scaling behavior:** $(2N)^{1/2}$ approached strictly from below
- **Computational complexity:** Exponential growth in configurations
- **Symmetry principles:** X-T symmetry constrains probabilities
- **Need for approximations:** Exact enumeration limited to small N

Layered Structure

- Causal sets exhibit natural layered organization
- Only fraction derivable from manifold sampling
- Weight construction becomes crucial for larger N

Layers Of Bricks Make A House

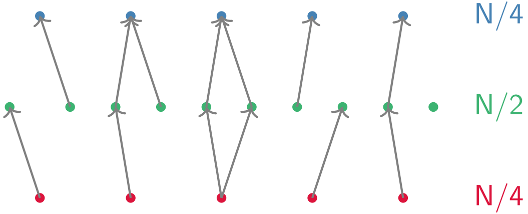

- Set P of N elements with partial order $\prec$
- Three-layer structure:
  - Top: $N/4$ elements
  - Middle: $N/2$ elements
  - Bottom: $N/4$ elements
- Only adjacent layers connected
- Relations understood by transitivity

Counting Partial Orders

Number of Connections

- Top to middle layer: $2^{N/4 \cdot N/2}$ ways
- Middle to bottom layer: $2^{N/2 \cdot N/4}$ ways
- **Total**: $2^{N^2/4}$ distinct partial orders

Modified Structure: Moving δ Nodes

When moving δ nodes from top to bottom:

$$2^{(N/4-\delta)(N/2)} \cdot 2^{(N/2)(N/4+\delta)} = 2^{N^2/4} \tag{19}$$

Same number of partial orders regardless of δ!

The Entropy Problem

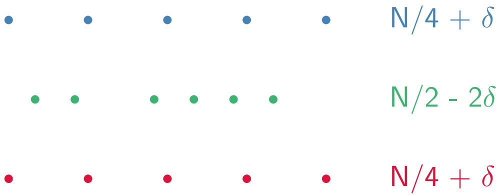

Key Issues

- Entropy $S \propto \log(\Omega) \propto N^2$
- **Not extensive!**
- Finite-layer posets are quadratic in N
- Need **infinite layers** for extensive entropy

A Challenge in Causal Set Theory

The Problem

If partial orders are fundamental building blocks of spacetime, how do we get manifold-like behavior?

Key Observations

- Sampling causal sets from manifolds gives partial orders with **extensive entropy**
- Expected from Poisson sampling: $\exp(N)$ configurations
- **Manifold-like** posets are exponentially rare among all posets

Proposed Solution

Assign **statistical weights** to each partial order configuration such that:

- Uniformly embeddable posets are more likely
- Expected sampled poset is manifold-like

A Statistical Approach

Probability Distribution

For configuration $\mathcal{C}$ of points and partial order relations:

$$\mathbb{P}(\mathcal{C}) = \frac{\exp(-\beta E_{\mathcal{C}})}{\mathcal{Z}} \tag{20}$$

where $\mathcal{Z} = \sum_{\mathcal{C}} \exp(-\beta E_{\mathcal{C}})$ is the partition function.

Energy Function

Need to define energy $E_{\mathcal{C}}$ such that:

- Energy ≈ 0 or negative for flat Lorentzian manifolds
- Energy large and positive otherwise

Constructing the Energy Function

Continuum Inspiration

In flat $(1+1)$-D spacetime: well-defined relation between proper time τ and causal volume V for causal diamonds.

Discrete Analogue

$$E_{\mathcal{C}} = \sum_{(a,b)\in\mathcal{C}}^{\text{all timelike pairs}} f(|[a,b]|, \tau_G(a,b)) \tag{21}$$

where:

- $|[a,b]|$ is the causal volume (number of elements in causal interval)
- $\tau_G(a,b)$ is the proper time between a and b

Harmonic Oscillator Approach

Quadratic Energy Function

$$f(V_{ab}, \tau_{ab}) = \frac{(V_{ab} - c_d \cdot \tau_{ab}^d)^2}{[\sigma(\tau_{ab})]^2} \tag{22}$$

- Working in $d-1$ spatial dimensions
- c_d is a constant (e.g., $c_2 = 1/2$ for 2D)
- $\sigma(\tau_{ab})$ determines fluctuation geometry

Result

Gaussian distribution of posets centered on those that are flat!

Choosing Fluctuations: Poisson Sprinkling

Poisson Statistics

- $\langle n \rangle = \rho V$
- $\mathrm{var}(n) = \rho V$

Final Energy Function

Choose variance as ρV_{ab}:

$$f(V_{ab}, \tau_{ab}) = \frac{1}{\rho} \frac{(V_{ab} - c_d \cdot \tau_{ab}^d)^2}{V_{ab}} \tag{23}$$

Redefine $\beta = \kappa\rho$ where:

- Infinite temperature $\leftrightarrow$ zero density
- Zero temperature $\leftrightarrow$ infinite density

Numerical Results

Simulation Findings

Running simulations for different values of κ:

- Causal set reduced from $\sim \sqrt{2N}$ layers to finite number
- Results in **three-layered structures** in large steps limit

The interpretation of this result is unclear at present but we expect that the energy function constructed is **wrong** because in the large-step limit it takes the system out from a manifold-like causet to a non-manifold-like poset.

The Apple and the Physicist

- Classical view: Apple falls to Earth
- Relativistic view: Earth falls toward apple too
- Modern understanding: **Both freely fall in curved spacetime**
- Curvature determined by the falling masses themselves

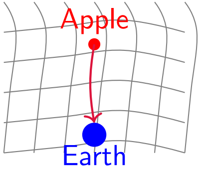

Diffeomorphism Invariance

Key Principle

In general relativity, **physical observables are independent of coordinates**

- Manifests locally as Lorentz invariance
- Global Lorentz invariance impossible due to curvature
- Extended through connections and parallel transport

Historical Context

General consensus linked Lorentz invariance and causality, but **Zeeman provided the first concrete proof**

Basic Definitions [8]

Consider an event-set M (discrete or manifold) with relations:

Relations

- **Chronological**: $x \ll y$
- **Causal**: $x \prec y$
- **Horismos**: $x \to y$ if $x \prec y$ but not $x \ll y$

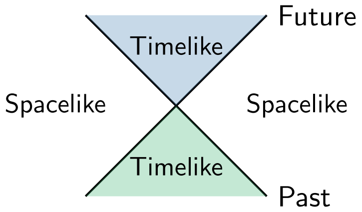

Lorentzian Manifold Structure

For smooth manifold X with Lorentzian metric:

- **Null cone** N_x: vectors with zero metric length
- Tangent vectors classified as:
  - Timelike (inside null cone)
  - Spacelike (outside null cone)
  - Null (on null cone)
- Decomposition into **future-directed** and **past-directed**

First Restriction

Manifold is **future-distinguishing** and **past-distinguishing**

Path Relations

From future/past distinction, define path orientations:

Relations

- xTy: positive timelike path from x to y
- xNy: positive non-spacelike path from x to y

Properties

For all $x, y, z \in X$:

1. If xTy, then xNy
2. If xNy and yNz, then xNz
3. If xTy and yNz, or if xNy and yTz, then xTz

Causal Space Definition

Second Restriction

Manifold is **causal**: no closed non-spacelike curves ($\neg xNx$)

Define relations:

$$x \prec y \iff xNy \text{ or } x = y \tag{24}$$

$$x \ll y \iff xTy \tag{25}$$

$$x \to y \iff (xNy \text{ and not } xTy) \text{ or } x = y \tag{26}$$

Important Caveat

Not every causal space is locally Minkowskian (Kronheimer & Penrose)

Abstract Causal Space

Tuple $(X, \prec, \ll, \rightarrow)$ is a **causal space** if for all $x, y, z \in X$:

1. $x \prec x$ (reflexive)
2. $x \prec y \wedge y \prec z \Rightarrow x \prec z$ (transitive)
3. $x \prec y \wedge y \prec x \Rightarrow x = y$ (antisymmetric)
4. $\neg(x \ll x)$ (anti-reflexive)
5. $x \ll y \Rightarrow x \prec y$
6. $x \prec y \wedge y \ll z \Rightarrow x \ll z$
7. $x \ll y \wedge y \prec z \Rightarrow x \ll z$
8. $x \rightarrow y \iff x \prec y \wedge \neg(x \ll y)$

- X: **underlying set**
- Relations: **causality** $(\prec)$, **chronology** $(\ll)$, **horismos** $(\rightarrow)$

Zeeman's Theorem [9]

Theorem

The group of chronological automorphisms $(Aut_{\ll}(\mathbb{M}^d))$ *on* $\mathbb{M}^d$ *for* $d > 2$ *is isomorphic to the group of inhomogeneous Lorentz transformations and dilations* $(Lor(\mathbb{M}^d))$*.*

Chronological Automorphism

Bijection $f : M \to M$ where both f and f^{-1} preserve chronology

- No assumption of linearity or continuity
- Pure causal structure preservation

Why Not 2 Dimensions?

Example (2D Counterexample)

In $\mathbb{M}^2$ with characteristic form $Q(x) = x_0^2 - x_1^2$:
Change coordinates:

$$y_0 = x_0 - x_1 \tag{27}$$

$$y_1 = x_0 + x_1 \tag{28}$$

Let f_0, f_1 be arbitrary nonlinear orientation-preserving homeomorphisms $\mathbb{R} \to \mathbb{R}$.
Then $f(x_0, x_1) = (f_0(y_0), f_1(y_1))$ is a chronological automorphism but **not a Lorentz transformation**.

Proof Strategy: Five Lemmas

Key Lemmas (Zeeman)

1. Preserves chronology $\iff$ preserves horismos
2. Maps light rays to light rays
3. Maps parallel light rays to parallel light rays
4. **Maps each light ray linearly** (excludes 2D case)
5. Maps parallel equal intervals to parallel equal intervals

Proof Completion

- Compose with translation to fix origin
- Decompose points as linear combinations of light rays
- Linearity follows from Lemma 4
- Null-cone preservation allows scalar multiplication

Futures and Pasts

Symbol	Name	Definition
$J^+(a)$	Causal future	$\{x : a \prec x\}$
$I^+(a)$	Chronological future	$\{x : a \ll x\}$
$C^+(a)$	Null future	$\{x : a \rightarrow x\} = J^+(a) \setminus I^+(a)$
$J^-(a)$	Causal past	$\{x : x \prec a\}$
$I^-(a)$	Chronological past	$\{x : x \ll a\}$
$C^-(a)$	Null past	$\{x : x \rightarrow a\} = J^-(a) \setminus I^-(a)$
$[p, q]$	Causal interval	$\{x : p \prec x \prec q\}$
$\langle p, q \rangle$	Chronological interval	$\{x : p \ll x \ll q\}$
$x \parallel y$	Spacelike	$\neg(x \prec y \vee y \prec x)$

Regularity Condition

Definition (Regular Causal Space)

For distinct points x_1, x_2, y_1, y_2 where $x_i \to y_j$ for each i, j:

$$\text{horismos orders } x_1, x_2 \iff \text{horismos orders } y_1, y_2$$

Geometric Interpretation

- Maps null geodesics of flat Minkowski to straight lines
- All four points must lie on same null geodesic if conditions satisfied
- Very strong constraint on causal structure

Lemma

If $x \prec y \prec z$ and $x \to z$, then $x \to y \to z$.

Distinguishing Properties

Definition

An anti-reflexive partial ordering $\ll$ is:

- **Future-reflecting**: $I^-(x) \subset I^-(y)$ whenever $I^+(x) \supset I^+(y)$
- **Weakly distinguishing**: $x = y$ if $I^+(x) = I^+(y)$ and $I^-(x) = I^-(y)$
- **Future-distinguishing**: $x = y$ whenever $I^+(x) = I^+(y)$
- **Full**: Dense chronological relations in both time directions

Important

These define the **first restriction** rigorously but don't automatically imply the **second restriction** (causality)

Three Construction Types

Kronheimer & Penrose construct causal spaces $\mathfrak{A}$, $\mathfrak{B}$, $\mathfrak{C}$:

$\mathfrak{A}$: From Horismos $\to$

$$x \prec^{\mathfrak{A}} y \iff \exists \text{ finite sequence } x \to u_1 \to \cdots \to u_n \to y \tag{29}$$

$$x \ll^{\mathfrak{A}} y \iff x \prec^{\mathfrak{A}} y \text{ and not } x \to y \tag{30}$$

Result: **Weakest** causal/chronological relations compatible with $\to$

$\mathfrak{B}$: From Chronology $\ll$

Two variants: weakly distinguishing ($\mathfrak{B}_W$) and future-reflecting ($\mathfrak{B}_+$)
Result: **Strongest** causal/horismotic relations compatible with $\ll$

$\mathfrak{C}$: From Causality $\prec$

$$x \to^{\mathfrak{C}} y \iff x \prec y \text{ and } \prec \text{ linearly orders } [u, v] \tag{31}$$

$$\text{whenever } [u, v] \text{ is proper subset of } [x, y] \tag{32}$$

$$x \ll^{\mathfrak{C}} y \iff x \prec y \text{ and not } x \to^{\mathfrak{C}} y \tag{33}$$

Key Results

$$\to^{\mathfrak{C}} = \bigcup \{\text{reg. hor} \mid \text{cau } \prec\} \tag{34}$$

$$\ll^{\mathfrak{C}} = \bigcap \{\text{reg. chr} \mid \text{cau } \prec\} \tag{35}$$

Neither chronology nor horismos are extremal (weakest/strongest)

Causal Topologies

Symbol	Name	Definition
$\mathcal{T}^*$	Alexandrov	From chronological relation $\ll$. Open sets: $I^-(x), I^+(x) \in \mathcal{T}^*$ for all x
$\mathcal{T}^+$	Causal	From causal relation $\prec$. Closed sets: $J^-(x)$ closed for all x
$\mathcal{T}^{\mathrm{man}}$	Manifold	Standard manifold topology (when applicable)

Note

Causal spaces not necessarily manifolds, so topologies may not be Hausdorff

Topological Results

Lemma

For manifold causal space X, equivalent conditions:

1. $\mathcal{T}^* = \mathcal{T}^{man}$
2. $(X, \mathcal{T}^*)$ *is Hausdorff*
3. *Local causal structure matches global structure*
4. *Strong chronological separation property*

Lemma

If $(X, \mathcal{T}^*)$ is Hausdorff and $\ll$ is full, then $\ll$ is future- and past-distinguishing.

Significance

Links topological and causal properties, providing tools for analyzing causal structure

The Hawking-King-McCarthy-Malament Theorem

Definition (Strong Causality)

A point p in a spacetime is said to be **strongly causal** if every neighborhood of p contains a subneighborhood such that no causal curve intersects it more than once.

All the events in a **strongly causal spacetime** are strongly causal.

Key insight: Strong causality prevents closed causal curves locally.

The Hawking-King-McCarthy-Malament Theorem [10, 11, 12, 13, 14]

Theorem (HKMM Theorem)

If a map $f_b : M_1 \to M_2$ is a chronology preserving bijection between two d-dimensional strongly causal spacetimes which are both future and past distinguishing, then these spacetimes are **conformally isometric** *when $d > 2$.*

Implications:

- Causal structure almost completely determines geometry
- Only conformal factor remains undetermined
- Dimension $d > 2$ is crucial

Extensions of the HKMM Theorem

Levichev's Result [15]:

- Causal bijection $\implies$ chronological bijection
- Causal structure determines metric up to conformal factor

Parrikar and Surya's Result [16]:

- Causal spaces and their topology contain information about spacetime dimension

Bottom line: Causal structure is remarkably rich and constraining!

The Topology Problem

Standard Approach:

- Treat spacetime as a manifold with standard (Euclidean) topology
- Assign Lorentzian metric to this manifold

The Issue:

- We don't capture the **actual local topology** [17, 18] of Lorentzian manifolds
- Spacetime is experimentally verified to be Lorentzian, not Euclidean

Finkelstein's Insight [19]

"The causal structure of spacetime is **9/10** of the spacetime"

What this means:

- Causal structure $\approx$ almost everything
- Volume element $\approx$ the remaining $1/10$
- Volume element fixes the conformal factor

Key idea: If causal structure is so rich, why not start with it?

The Causal Set Proposal

Central Idea:

1. Start with a causal space (just a set with causal relations)
2. Fix volume element using **cardinality** of the set
3. This defines a $\mathfrak{C}$-space

The Setup:

- Discrete set of events
- Causal relations between events
- Number of events $\propto$ spacetime volume

Why Causal Sets?

Four Major Benefits:

1. **Natural Extension:** Continuum spacetime emerges as a **full extension** of the discrete set
2. **Tractable Topology:** Discrete topology is much easier to handle than continuum topology
3. **Statistical Methods:** Can study how metric **emerges statistically** from causal structure
4. **Sensible Path Integrals:** Discrete events may finally make path integrals well-defined

Three Fundamental Questions

To make causal sets work, we need to address:

1. **Manifold-like Causal Sets:**
   How to find causal sets that look like manifolds when extended?

2. **Lorentz Invariance:**
   How to maintain Lorentz invariance in a discrete causal set?

3. **Non-Lorentzian Possibilities:**
   Are there causal sets that are not Lorentzian manifolds?

The Setup:

- Given causal set C with N elements
- Want to embed in Lorentzian manifold M
- Think of points as **randomly sampled** from M

The Problem:

- Not all N-element posets look like manifolds
- Example: trivial chain $1 \prec 2 \prec \cdots \prec N$
- This is just a time axis - no spatial structure!

Question: What's the right probability distribution for sampling?

Faithful Embedding

Definition (Faithful Embedding)

A causal set $\mathcal{C}$ approximates spacetime $\mathcal{C} \sim (M, g)$ at **density** $\rho_c = V_c^{-1}$ if there exists a faithful embedding $p : \mathcal{C} \to M$ such that $p(\mathcal{C})$ is **uniformly distributed** over the spacetime volume measure of M.

Key Parameters:

- V_c: discretization scale
- ρ_c: sprinkling density
- Uniform distribution preserves spacetime symmetries on average

Poisson Process Sampling

Why not regular lattices?

- Break continuous symmetries $\to$ discrete symmetries
- We want to preserve Lorentz invariance!

Poisson Process Benefits:

- Preserves continuous symmetries **on average**
- Standard deviation: $\sigma = 1/\sqrt{\rho V}$
- For large V: $\sigma \to 0$ (very uniform)

Inspired by Christ, Friedberg, and Lee's random lattice field theory [20, 21, 22]. This is used in lattice gauge theory frequently [23, 24].

The Void Problem

Poisson Process Issue: In infinite volume, probability of finding voids of any size $= 1$

Three Possibilities:

1. Universe is infinite $+$ filled with voids (we're lucky)
2. Universe is finite (probability of nuclear void $\sim 10^{-10^{72}}$ [25])
3. Infinite universe with no voids on average

[Note: Need to discuss with professor!]

Emergence of Non-Locality

Key Issue

Major caveat in uniformly sampling a causal set via a Poisson process

- Consider element a in causal set $\mathcal{C}$
- Probability that event $x \in \mathcal{C}$ is a **link** equals:

  Probability that Alexandrov interval between a and x contains only a and x
- This probability depends on the **volume** of the Alexandrov interval

Goal

Compute this probability exactly for d-dimensional Minkowski spacetime

2D Minkowski Spacetime

- Point a at origin
- Point x at coordinates $(t, x_1) = (x_0, x_1)$
- Alexandrov interval = intersection of light cones
- **Blue region**: Alexandrov interval
- **Red lines**: Past light cone of x

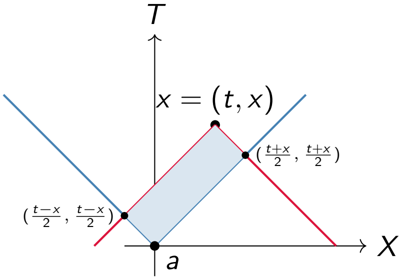

Volume Calculation: 2D Case

Volume of Alexandrov Interval

$$V(t,x) = 2 \times \left| \frac{1}{2} \frac{(t-x)}{2} (x-t) \right| + |x \times (t-x)| \tag{36}$$

$$= \frac{t^2 - x^2}{2} \tag{37}$$

Generalization: Modified Light Cone

For opening angle θ instead of $\pi/4$:

$$V(t,x) = \frac{t^2 \tan(\theta)}{2} - \frac{x^2}{2\tan(\theta)} \tag{38}$$

Higher Dimensions: Modified Lorentz Transformation

Setup

- d spatial dimensions
- Modified light cone: $|\mathbf{r}| = \pm \tan(\theta) t$
- Need linear transformation $\Lambda_{\text{mod}} : (t, |\mathbf{r}|) \to (t', |\mathbf{r}'|)$ such that $|\mathbf{r}'| = \pm \tan(\theta) t'$

The Complete Transformation

Modified Lorentz Transformation

$$\left|\mathbf{r}'\right| = \frac{|\mathbf{r}| - \omega t}{\sqrt{1 - \omega^2 \cot^2(\theta)}} \tag{39}$$

$$t' = \frac{t - \omega \cot^2(\theta)\,|\mathbf{r}|}{\sqrt{1 - \omega^2 \cot^2(\theta)}} \tag{40}$$

- Set $|\mathbf{r}'| = 0$ by choosing $|\mathbf{r}| = \omega t$
- Volume becomes two double cones of height $t'/2$ and base angle θ
- This gives us:

$$t' = \left(t^2 - |\mathbf{r}|^2 \cot^2(\theta)\right)^{1/2} \tag{41}$$

Volume Formula in d Dimensions

Alexandrov Interval Volume

$$\text{Vol}_d(t, |\mathbf{r}|) = \frac{\pi^{d/2}}{(d+1)\cdot\Gamma(\frac{d}{2}+1)} \cdot \frac{(t^2 - |\mathbf{r}|^2 \cot^2(\theta))^{(d+1)/2}}{2^d} \cdot \tan^d(\theta) \qquad (42)$$

Special Case: $\theta = \pi/4$

- $\cot(\theta) = \tan(\theta) = 1$
- Formula reduces to dimension-dependent scaling of metric interval
- Recovers standard Minkowski spacetime result

Next Step

Use this to find the probability of a link between events

Probability of a Link

Link Probability Formula

$$P(a \to x) = \exp\left(-\rho_c \cdot \mathrm{Vol}(t, |\mathbf{r}|)\right) \tag{43}$$

Significant Region

- Link probability significant when $\mathrm{Vol}_d(t, |\mathbf{r}|) < V_c$
- Region: **light cone minus hyperboloid of radius** V_c

Total Linking Volume

Up to height T:

$$\mathrm{Vol.(link)} = \frac{\pi^{d/2}}{(d+1)\cdot\Gamma(\frac{d}{2}+1)} \cdot T^{d+1} - \mathrm{Vol.(hyperboloid)} \tag{44}$$

Computing the Hyperboloid Volume

Hyperboloid Definition

Region defined by: $t^2 - \mathbf{r}^2 \geq V_c^2$ with $t \in [V_c, T]$

Spatial Slices

At fixed time $t > V_c$:

- Constraint: $\mathbf{r}^2 \leq t^2 - V_c^2$
- d-dimensional ball of radius $R(t) = \sqrt{t^2 - V_c^2}$
- Volume: $\mathrm{Vol}_d(R(t)) = \frac{\pi^{d/2}}{\Gamma(\frac{d}{2}+1)} \left(t^2 - V_c^2\right)^{d/2}$

Total Spacetime Volume

$$\mathrm{Vol}_{d+1}(V_c, T) = \int_{V_c}^{T} \frac{\pi^{d/2}}{\Gamma\left(\frac{d}{2}+1\right)} \left(t^2 - V_c^2\right)^{d/2} dt \tag{45}$$

Solving the Integral

Substitution

Let $t = V_c \cosh u$, so $dt = V_c \sinh u \, du$

Transformed Integral

$$\text{Vol(hyperboloid)} = \frac{\pi^{d/2}}{\Gamma\left(\frac{d}{2}+1\right)} \int_0^{\cosh^{-1}(T/V_c)} (V_c \sinh u)^{d+1} \, du \tag{46}$$

$$= \frac{\pi^{d/2} V_c^{d+1}}{\Gamma\left(\frac{d}{2}+1\right)} \int_0^{\cosh^{-1}(T/V_c)} \sinh^{d+1} u \, du \tag{47}$$

Key Observation

$\frac{d}{dT}\text{Vol(link)} > 0$ - monotonically increasing function!

Critical Result

- Vol(link) increases monotonically with T
- Possible region for links is **infinite**
- We will **surely find a link** in the infinite future

Important Takeaway

- Links are nearest neighbors of each other
- This implies **infinitely many links** in the far future
- Results in **emergent non-locality** in the causal set [26]

Invariance in Random Sampling

Why do Euclidean and Lorentzian manifolds behave differently under random sampling?

Symmetry Preservation Principle

Main Result

Random uniform sampling from a manifold preserves continuous symmetries **on average** when the symmetry group is **compact**.

Euclidean Case [27]

- Symmetry group: compact
- Individual realizations break symmetry
- Ensemble average preserves symmetry

Lorentzian Case [28]

- Symmetry group: non-compact (boosts)
- Individual realizations preserve symmetry
- Different mechanism at work

Euclidean Example: $\mathbb{R}^2$

Breaking Rotational Symmetry

Setup

- Plane $\mathbb{R}^2$ with Euclidean metric
- Embedding map: $p : \mathcal{C}(\mathbb{R}^2, \rho) \to \mathbb{R}^2$
- $\mathcal{C}(\mathbb{R}^2, \rho)$: ensemble of Poisson sprinklings at density ρ

Symmetry Actions

- Rotations: $r \in SO(2)$ induce $r^* = p^{-1} \circ r \circ p$
- Translations: $t \in \mathbb{R}^2$ induce $t^* = p^{-1} \circ t \circ p$
- Unit vectors lie on S^1 (compact)

Direction Assignment

For point $e \in p(P)$: direction $\mathbf{d}$ = vector from e to closest neighbor
Define direction map: $\mathbf{D}_e : \mathcal{C}(\mathbb{R}^2, \rho) \to S^1$

Probability Measures and Invariance

Measure Theory

- Poisson process induces probability distribution μ on $\mathcal{C}(\mathbb{R}^2, \rho)$
- Volume preserving: $\mu = \mu \circ r$ (invariant under rotations)
- Induced measure on S^1: $\mu_{\mathbf{D}} = \mu \circ \mathbf{D}^{-1}$

Key Property

Direction map commutes with rotations: $\mathbf{D}_e \circ r^* = r \circ \mathbf{D}_e$
Therefore: $\mu_{\mathbf{D}}$ is invariant under $SO(2)$ action

Symmetry Breaking

- S^1 is compact $\Rightarrow$ can partition into n equal measurable sets $A_1, \ldots, A_n$
- Each has measure $\mu_{\mathbf{D}}(A_i) = \frac{1}{n}$
- **Consistent direction assignment possible**

Lorentzian Manifolds: The Difference

Critical Differences

1. Symmetry group is **non-compact** (includes boosts)
2. Directions lie on **hyperboloid** (non-compact)
3. Poisson sampling still preserves volume measure

The Impossibility Argument

Assume consistent direction map exists for Lorentzian case:

- Try to partition hyperboloid into equal measurable sets
- If possible: $\mu_{\mathbf{D}}(A_i) = 0$ for all i, but sum must equal 1
- **Contradiction!**

Conclusion

Cannot consistently assign directions in Lorentzian manifolds
$\Rightarrow$ **Continuous symmetries NOT broken** by Poisson process

Why Lorentzian Symmetries Survive

Reason 1: Non-Compact Symmetry Group

Lorentz group $SO(1, d-1)$ includes boosts $\Rightarrow$ non-compact

Reason 2: Non-Compact Direction Space

Directions lie on hyperboloid, not sphere $\Rightarrow$ non-compact manifold

Reason 3: Volume Preservation

Poisson sampling preserves volume measure $\Rightarrow$ maintains statistical invariance

Implication

Every realization of Poisson process on Lorentzian manifold preserves continuous symmetries

$\Rightarrow$ **Local Lorentz invariance emerges naturally**

Beyond Poisson: Alternative Distributions

Open Question

Do distributions other than Poisson also preserve volume?

If Yes, Then:

- Would also predict local Lorentz invariance
- Opens door to richer variety of statistics
- Could potentially address non-locality issues

Optimization Criterion

Most suitable distributions would be those that:

- Preserve volume measure
- **Minimize fluctuations**
- Maintain causal structure

Euclidean vs Lorentzian: Summary

Property	**Euclidean**	**Lorentzian**
Symmetry Group	Compact	Non-compact
Direction Space	S^{d-1} (compact)	Hyperboloid (non-compact)
Individual Realization	Breaks symmetry	Preserves symmetry
Ensemble Average	Preserves symmetry	Preserves symmetry
Direction Assignment	Possible	Impossible
Mechanism	Statistical averaging	Geometric constraint

Key Insight

The **compactness** of the symmetry group determines whether individual realizations can break continuous symmetries while preserving them on average.

Counting Posets: The Problem [29, 30]

- **Goal:** Count the number of posets with n elements
- **Motivation:** Essential for constructing path integrals on the space of all posets
- Entropy of non-manifold-like posets cannot be ignored
- Connection to finite topologies via Kleitman-Rothschild work

Key Question

How does the number of n-element posets grow with n?

Equivalent Enumeration Problems

For a set X with n elements, define:

$$T_n = |T(X)| \quad \text{(all topologies)} \tag{48}$$
$$P_n = |P(X)| \quad \text{(partial orders)} \tag{49}$$
$$T_{n,0} = |T_0(X)| \quad (T_0\text{-topologies}) \tag{50}$$
$$O_n = |O(X)| \quad \text{(preorders)} \tag{51}$$

Theorem (Equivalence)

$T_n = O_n$, $T_{n,0} = P_n$, and all eight quantities (including isomorphism classes T'_n, P'_n, etc.) have asymptotically equal logarithms.

Key insight: Topology counting reduces to poset counting via closure operators.

Bounds on the Number of Posets

Theorem (Lower Bound)

$P_n \geq 2^{n^2/4}$

Theorem (Upper Bound)

For some constant C:

$$\log P_n \leq \frac{n^2}{4} + Cn^{3/2} \log n$$

Interpretation

- Entropy grows **quadratically** in n
- Much faster than linear growth expected from Poisson processes
- Indicates complex kinematics of causal sets

Proof Strategy for Upper Bound

Classify Hasse diagrams into four types based on vertex connectivity:

- Type A: Each vertex adjacent to $\leq (n-1)/64$ others
- Type B: Minimal element covered by $\lfloor n^{1/2} \rfloor$ vertices, with $|N(Q)| \geq n/2$
- Type C: Minimal element covered by $\lfloor n^{1/2} \rfloor$ vertices, with $|N(Q)| \leq n/2$

Key Lemmas

$$\log(A_{n+1}/P_n) < n/5 \tag{52}$$

$$\log(B_{n+1}/P_n) < n/2 + n^{1/2} \log n \tag{53}$$

$$\log(C_{n+1}/P_{n-\lfloor n^{1/2} \rfloor}) \leq n^{3/2}/2 + 4n \tag{54}$$

Implications for Causal Set Theory

- **Entropy scaling:** $\log P_n \sim n^2/4$ (quadratic, not linear)
- Path integral over posets requires careful treatment of entropy
- Non-manifold-like configurations contribute significantly
- Need formalized notion of entropy on posets (Dhar's approach)

Next Steps

1. Dhar's entropy construction on poset structures
2. First-order phase transitions
3. Higher-order modifications and numerical results

Entropy With Constraints [31]

Define entropy as $S = \lim_{n\to\infty} \frac{2}{n^2} \ln P_n$, giving $S = \frac{1}{2}\ln 2$.
For posets with fraction ρ of comparable pairs: $S(\rho) = \lim_{n\to\infty} \frac{2}{n^2} \ln P_n(\rho)$

Theorem (Entropy Properties)

- $S(0) = S(1) = 0$ *and* $S(\rho) \leq \frac{1}{2}\ln 2$
- $S(\rho)/\rho$ *is monotonic non-increasing*
- $S(\rho)/(1-\rho)$ *is monotonic non-decreasing*
- $S(\rho)$ *is continuous on* $[0, 1]$

Key insight: These properties constrain the possible form of $S(\rho)$.

Layered Poset Variational Model

Consider r layers with f_i fraction of elements in layer i, and α fraction of adjacent-layer pairs comparable.

Constraint Equation

$1 - \rho = \sum_{i=1}^{r} f_i^2 + 2(1-\alpha) \sum_{i=1}^{r-1} f_i f_{i+1}$

Entropy Lower Bound

$S(\rho) \geq 2B \cdot \mathcal{S}(\alpha)$ where $B = \sum_{i=1}^{r-1} f_i f_{i+1}$ and $\mathcal{S}(\alpha) = -\alpha \ln \alpha - (1-\alpha)\ln(1-\alpha)$.

Maximum entropy requires $B = 1/4$ and $\alpha = 1/2$.

Theorem (Maximum Entropy Plateau)

$S(\rho_0) = \frac{1}{2}\ln 2$ *for* $\rho_0 \in [5/8, 3/4]$ *where* $\rho_0 = 1 - \rho$.

Phase Transition Structure

- For $\rho_0 < 5/8$: $S(\rho_0) \geq \frac{4}{5}\rho_0 \ln 2$
- For $\rho_0 > 3/4$: $S(\rho_0) = \frac{1}{2}\mathcal{S}(2(1-\rho_0))$
- Transitions occur when optimal layer number changes
- First-order: entropy continuous but derivative discontinuous

Physical interpretation: Density of comparable pairs drives phase transitions, measurable via chemical potential.

Variational Analysis

Lagrangian for maximizing entropy lower bound:

$$\mathcal{L} = 2B \cdot \mathcal{S}(\alpha) + \lambda_1 \left(1 - \sum f_i\right) + \lambda_2(\rho_0 - A - 2(1-\alpha)B) \tag{55}$$

Solution structure: symmetric about middle layer, leading to 3-layer optimal configurations for intermediate ρ_0.

Result: Infinite sequence of first-order phase transitions as optimal layer number changes.

Connection to Lattice Gas Model

- $\binom{n}{2}$ lattice sites, each with 3 states (unoccupied, relation in either direction)
- Transitivity constraint creates 3-body interactions
- **Non-locality:** "Strong, long range nature of 3-body interaction"
- Fundamental to causal set theory due to null geodesic non-locality

Kleitman-Rothschild Result

For $\rho_0 > 3/4$, two layers are sufficient to describe optimal posets.

How the entropy looks

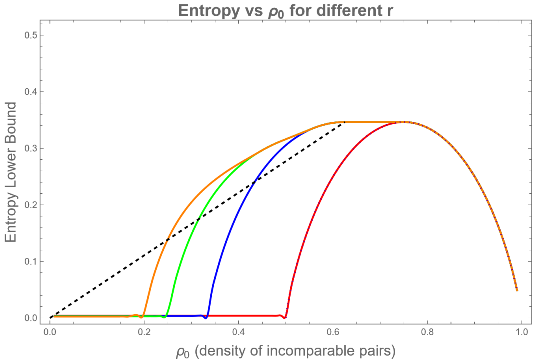

Figure: The variational entropy function $S(\rho_0)$ as a function of the density of incomparable pairs ρ_0, for different r. The envelope of these curves is the entropy function $S(\rho_0)$, which is continuous and has an infinite number of first order phase transitions. The dashed line is the lower bound upto $\rho_0 = 5/8$, and the dotted curve is the lower bound for $\rho_0 > 3/4$.

Entropy With Constraints - II

- We investigate **phase transitions** in the entropy as a function of:
  - Density of incomparable pairs (ρ_0)
  - Density of links (ρ_1)
- Goal: Generalize beyond single parameter variations
- Key insight: $\rho_1 = 2\alpha B$ where α and B are defined parameters
- Analyze the $\rho_0 - \rho_1$ plane for entropy structure

Entropy Function Definition

The entropy function is defined as:

$$S(\rho_0, \rho_1) = \lim_{n\to\infty} \frac{2}{n^2} \ln P_n(\rho_0, \rho_1) \tag{56}$$

$$S_{\text{var}}(\rho_0, \rho_1) = 2B \cdot \mathcal{S}(\alpha) \tag{57}$$

where $\mathcal{S}(\alpha) = -\alpha \ln \alpha - (1-\alpha)\ln(1-\alpha)$ is the **binary entropy function**.

Parameter Relations

The densities are expressed in terms of layer parameters:

$$\rho_0 = A + 2(1-\alpha)B \tag{58}$$

$$\rho_1 = 2\alpha B \tag{59}$$

where:

$$A = \sum_{i=1}^{r} f_i^2 \tag{60}$$

$$B = \sum_{i=1}^{r-1} f_i f_{i+1} \tag{61}$$

Subject to constraints:

$$\sum_{i=1}^{r} f_i = 1, \quad f_i \geq 0, \quad \alpha \in (0,1) \tag{62}$$

Key Monotonicity Results

Lemma 1: Monotonicity in ρ_1

For fixed ρ_0:

- $S(\rho_0, \rho_1)/\rho_1$ is **monotonic non-decreasing** in ρ_1
- $S(\rho_0, \rho_1)/(1 - \rho_1)$ is **monotonic non-increasing** in ρ_1

Lemma 2: Continuity

$S(\rho_0, \rho_1)$ is a **continuous function** of both ρ_0 and ρ_1.

Lagrangian Optimization

To find maximum entropy configurations:

$$\mathcal{L} = S_{\text{var}}(\rho_0, \rho_1) + \lambda_1 \left(1 - \sum_{i=1}^{r} f_i\right) \tag{63}$$

$$+ \lambda_2 \left(\rho_0 - A - 2(1-\alpha)B\right) \tag{64}$$

$$+ \lambda_3 \left(\rho_1 - 2\alpha B\right) \tag{65}$$

Critical equations:

$$\frac{\partial \mathcal{L}}{\partial \alpha} = 0 \implies 2B\left(\ln\left(\frac{1-\alpha}{\alpha}\right) + \lambda_2 - \lambda_3\right) = 0 \tag{66}$$

$$\frac{\partial \mathcal{L}}{\partial f_i} = 0 \implies \text{coupling between adjacent layers} \tag{67}$$

Two-Layer Posets

For $f_1 = f$, $f_2 = 1 - f$:

$$\rho_0 = f^2 + (1-f)^2 + 2(1-\alpha)f(1-f) \tag{68}$$

$$\rho_1 = 2\alpha f(1-f) \tag{69}$$

- **Constraint**: $\rho_0 + \rho_1 = 1$ (elements are either comparable or linked)
- Minimum $\rho_0 = 1/2$ at $\alpha = 1$, $f = 1/2$
- Maximum $\rho_1 = 1/2$ at same point
- **Maximum entropy** at $\rho_0 = 3/4$, $\rho_1 = 1/4$

Three-Layer Posets

For $f_1 = x$, $f_2 = y$, $f_3 = 1 - x - y$:

$$\rho_0 = x^2 + y^2 + (1 - x - y)^2 + 2(1 - \alpha)(xy + y(1 - x - y)) \tag{70}$$

$$\rho_1 = 2\alpha(xy + y(1 - x - y)) = 2\alpha y(1 - y) \tag{71}$$

- Maximum $\rho_1 = 1/2$ at $\alpha = 1$, $y = 1/2$
- Minimum $\rho_0 = 1/3$ with equal layer fractions and $\alpha = 1$
- **Allowed region**: $1/2 < \rho_0 + \rho_1 < 1$
- Zero entropy at $(\rho_0, \rho_1) = (1/3, 4/9)$

Linear Bounds for Three-Layer Posets

Analysis of $\rho_0 + \xi\rho_1$:

$$\rho_0 + \xi\rho_1 = 2x^2 - 2x + 2xy + 1 \tag{72}$$
$$+ 2\alpha(\xi - 1)(y - y^2) \tag{73}$$

- $\xi = 1$: bounds $1/2 < \rho_0 + \rho_1 < 1$
- $\xi = 1/2$: bound $\rho_0 + \frac{1}{2}\rho_1 > 1/2$
- Function $f(x, y) = 2x^2 - 2x + 2xy + 1$ has range $(1/2, 1)$

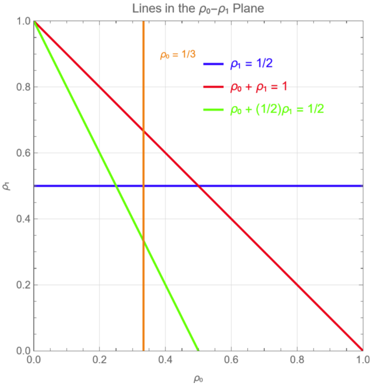

Figure: Theoretical Bounds on 3-layer

Entropy Landscape for Three Layers

- **Maximum entropy**: $\frac{1}{2}\ln 2$
- Achieved for $y = 1/2$, $\alpha = 1/2$
- Range: $\rho_0 \in [5/8, 3/4]$
- Entropy function is continuous in allowed region
- **First-order** phase transitions

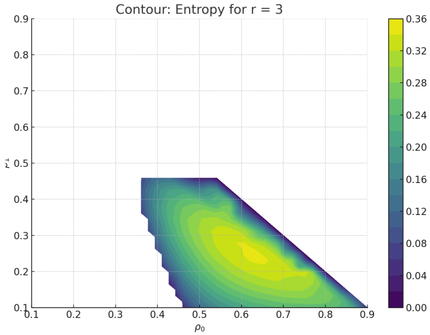

Figure: Entropy for 3-layer

Higher Layer Posets

- **Analytic bounds** difficult for $r > 3$ layers
- Numerical evidence suggests **expanding regions**
- Same (ρ_0, ρ_1) can support multiple layer configurations
- Entropy remains continuous across regions
- Phase transitions remain **first-order**

Critical Observation

Transition curves between r and $r + 1$ layers are **not** critical points of the entropy function!

Special Case: $y = 1/2$ in Three Layers

When middle layer has half the elements:

$$\rho_0 + \rho_1 = x^2 + \left(\frac{1}{2} - x\right)^2 + \frac{3}{4} \in \left(\frac{7}{8}, 1\right) \tag{74}$$

- Constraint: $\alpha = 2\rho_1$ (minimum value)
- For $\rho_0 \in (3/8, 1/2)$: entropy follows **two-layer formula**
- $S = \frac{1}{2}\mathcal{S}(2\rho_1)$
- Transition between 2 and 3 layers occurs in $\rho_0 \in (3/4, 7/8)$

Key Results

1. **Monotonicity properties** established for entropy in ρ_0-ρ_1 plane
2. **Continuous entropy function** with well-defined domains
3. **First-order phase transitions** between different layer configurations
4. **Maximum entropy** configurations identified for specific cases
5. **Complex phase structure** emerges for higher-layer systems

Example: $\mathbb{Z}^2$ directed percolation

We hope to extract a Lorentzian metric on directed percolation models.

References I

Luca Bombelli, Joohan Lee, David Meyer, and Rafael D. Sorkin.
Spacetime as a causal set.
Phys. Rev. Lett., 59:521–524, 1987.

Cristopher Moore.
Comment on "space–time as a causal set".
Phys. Rev. Lett., 60:655–656, 1988.

Luca Bombelli and David A. Meyer.
The origin of lorentzian geometry.
Phys. Lett. A, 141:226–228, 1989.

Steven Johnston.
Embedding causal sets into minkowski spacetime.
Classical and Quantum Gravity, 39(9):095006, may 2022.

References II

Steven Johnston.
Simpler embeddings of causal sets into minkowski spacetime.
Phys. Rev. D, 111:106020, May 2025.

D. A. Meyer.
The dimension of causal sets.
PhD thesis, M.I.T., 1988.

David D. Reid.
Manifold dimension of a causal set: Tests in conformally flat spacetimes.
Phys. Rev. D, 67:024034, Jan 2003.

E. H. Kronheimer and R. Penrose.
On the structure of causal spaces.
Mathematical Proceedings of the Cambridge Philosophical Society, 63(2):481–501, 1967.

References III

E. C. Zeeman.
Causality implies the lorentz group.
Journal of Mathematical Physics, 5(4):490–493, 04 1964.

S. W. Hawking, A. R. King, and P. J. McCarthy.
A new topology for curved space–time which incorporates the causal, differential, and conformal structures.
Journal of Mathematical Physics, 17(2):174–181, 02 1976.

Stephen W. Hawking and George F. R. Ellis.
The Large Scale Structure of Space-Time: 50th Anniversary Edition.
Cambridge Monographs on Mathematical Physics. Cambridge University Press, 2023.

References IV

David B. Malament.
Causal theories of time and the conventionality of simultaneity.
Noûs, 11(3):293–300, 1977.

David B. Malament.
The class of continuous timelike curves determines the topology of spacetime.
Journal of Mathematical Physics, 18(7):1399–1404, 1977.

David B. Malament.
Observationally indistinguishable space-times.
In John Earman, Clark Glymour, and John Stachel, editors, *Foundations of Space-Time Theories*, volume 8 of *Minnesota Studies in the Philosophy of Science*, pages 61–80. University of Minnesota Press, Minneapolis, 1977.
Online resource (PDF).

A. V. Levichev.
The causal structure of a lorentzian manifold determines its conformal geometry.
Dokl. Akad. Nauk SSSR, 293(6):1301–1305, 1987.
MathNet link, MathSciNet: MR891556, Zbl 0637.53077.

Onkar Parrikar and Sumati Surya.
Causal topology in future and past distinguishing spacetimes.
Classical and Quantum Gravity, 28(15):155020, jul 2011.

E.C. Zeeman.
The topology of minkowski space.
Topology, 6(2):161–170, 1967.

Giacomo Dossena.
Some results on the zeeman topology.
Journal of Mathematical Physics, 48(11):113507, 11 2007.

References VI

David Finkelstein.
Space-time code.
Phys. Rev., 184:1261–1271, Aug 1969.

Friedberg R Christ, N H and T D Lee.
Random lattice field theory. general formulation.
Nucl. Phys. B, 202:1.

C. Itzykson.
Fields on a Random Lattice.
Springer US, Boston, MA, 1984.

T. D. Lee.
CAN TIME BE A DISCRETE DYNAMICAL VARIABLE?
Phys. Lett. B, 122:217, 1983.

N.H. Christ, R. Friedberg, and T.D. Lee.
Gauge theory on a random lattice.
Nuclear Physics B, 210(3):310–336, 1982.

N.H. Christ, R. Friedberg, and T.D. Lee.
Weights of links and plaquettes in a random lattice.
Nuclear Physics B, 210(3):337–346, 1982.

FAY DOWKER, JOE HENSON, and RAFAEL D. SORKIN.
Quantum gravity phenomenology, lorentz invariance and discreteness.
Modern Physics Letters A, 19(24):1829–1840, 2004.

Sumati Surya.
The causal set approach to quantum gravity.
Living Reviews in Relativity, 22(1):5, 2019.

References VIII

Dietrich Stoyan, Wilfrid S. Kendall, and Joseph Mecke.
Stochastic Geometry and Its Applications.
Wiley, Chichester, 1995.

Luca Bombelli, Joe Henson, and Rafael D. Sorkin.
Discreteness without symmetry breaking: A theorem.
Modern Physics Letters A, 24(32):2579–2587, 2009.

D. Kleitman and B. Rothschild.
The number of finite topologies.
Proceedings of the American Mathematical Society, 25(2):276–282, 1970.

D. J. Kleitman and B. L. Rothschild.
Asymptotic enumeration of partial orders on a finite set.
Transactions of the American Mathematical Society, 205:205–220, 1975.

Deepak Dhar.
Entropy and phase transitions in partially ordered sets.
Journal of Mathematical Physics, 19(8):1711–1713, 08 1978.

Thank you for listening

Questions?